Geometrical and electronic structure of the reconstructed diamond (100) surface

C. Kress, M. Fiedler, W.G. Schmidt, and F. Bechstedt
Institut für Festkörpertheorie und Theoretische Optik, Friedrich-Schiller-Universität,
Max-Wien-Platz 1, 07743 Jena, Germany
(Received 10 August 1994)

We present the result of fully self-consistent ab initio density-functional calculations for clean C(100) surfaces. Studying 2×2 and 2×1 reconstructed surfaces, we find the symmetric dimer 2×1 geometry to be the ground state. The corresponding electronic band structure is calculated within the GW approximation, i.e., many-body quasiparticle effects are included.

Recently the diamond (100) surface has attracted new interest due to the challenging technological advances of nearly atomically smooth thin-film growth of this surface by chemical vapor deposition (CVD) methods.^{1,2} There are several theoretical studies of the structural and electronic properties of this surface.3-7 The level of sophistication ranges from SLAB-MINDO (modifiedintermediate-neglect-of-differential-overlap) (Ref. 4) and empirical tight-binding methods (ETBM)^{3,5} to non-selfconsistent calculations using density-functional theory (DFT).^{6,7} Despite these investigations concerning the structural properties of the clean diamond (100) surfaces there is still an ongoing debate on the particular geometry of this surface. By analogy to silicon (100) symmetric and asymmetric dimer reconstructions are discussed. An open question is, if there exist higher reconstructions at low temperatures, such as the $c(2\times4)$ one in the Si(100) case.8 Furthermore, substantial discrepancies remain with respect to the dimer bonding and the energetics between the different approaches. Low-energy electron-diffraction¹ and scanning-tunneling microscopy^{7,9} find a 2×1 reconstruction when the temperature is elevated to about 1300 K. Apart from results of few theoretical studies the electronic properties of the C(100) surfaces are rather unknown. Neither the appearance of surface states in the fundamental gap nor their dispersion are studied. Because of the experimental complications with the polycrystalline CVD films angleresolved photoemission or inverse photoemission measurements have not been made. Also the STM has not been used yet for spectroscopic studies. Thus there is a challenge for theoretical state-of-the-art calculations of both the geometrical and electronic properties of this surface.

In this paper we report the first fully self-consistent ab initio pseudopotential calculations for C(100) surfaces. Using the density-functional theory (DFT) within the local-density approximation (LDA), total energy calculations are performed for various structural models in order to determine the atomic positions of the atoms at the surface. 2×2 and 2×1 surface reconstructions are considered. For the correct calculation of the electronic properties we go beyond the DFT-LDA applying the quasiparticle (QP) theory to include the many-body effects of exchange and correlation in a proper way. The QP band structure presented is calculated by means of a computationally scheme using the GW approximation of the

self-energy.

The details of the DFT-LDA calculations are like those in Ref. 10. The electron-ion interaction is treated by using norm-conserving, ab initio, fully separable pseudopotentials.¹¹ The pseudopotential for carbon has been softened as described in Ref. 10. The electron-electron interaction in LDA is treated within the Ceperley-Alder scheme. 12 We use the repeated-slab method to simulate the surfaces. A single slab contains 12 (100) layers of carbon atoms and a vacuum region equivalent in thickness to 12 such layers. The planewave basis set is restricted by an energy cutoff equal to 34 Ry. In a detailed convergence study¹⁰ this energy cutoff together with the softened C pseudopotential has been proofed to give accurate results for bulk SiC properties. The k-space integration is replaced by a sum over four special points in the irreducible part of the surface Brillouin zone (SBZ). In order to determine the equilibrium positions, the atoms of the four innermost substrate layers are kept frozen at their ideal positions, whereas all other atoms are allowed to relax until the total energy and the forces are minimized. Simultaneously with the relaxation of the ions the single-particle wave functions are brought to self-consistency within a Car-Parrinello-like minimization scheme of the total energy functional¹³ using a modified computer code of Stumpf and Scheffler. 14

In order to obtain reliable geometrical data we minimize the total energy of several atomic arrangements. These are symmetric and asymmetric dimer 2×1 reconstructions of the (100) surface as well as a 2×2 surface reconstruction containing two oppositely buckled dimers. All these starting configurations relax to the same 2×1 reconstructed surface which is characterized by a symmetrically dimerized geometry in the top layer. This finding is in contrast to the ab initio DFT-LDA results for the Si(100)2×1 surface, 8,16,17 which have indicated a dimer buckling with a tilt angle of 14°-17°. A possible reason is the tendency of the carbon atoms to form double bonds even at the surface. The energy gain due to the formation of a C=C double bond instead of a single bond as in the silicon case is larger than that due to the charge transfer between the inequivalent dimer atoms.

A side view of the resulting surface structure is shown in Fig. 1. The geometry parameter are listed in Table I. In close agreement to Ref. 4 we find the bond length of the carbon dimer at the surface with 1.37 Å slightly

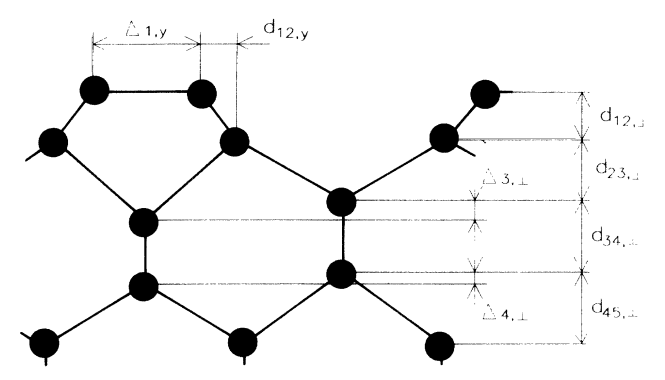


FIG. 1. Side view of the reconstructed $C(100)2\times 1$ surface. The corresponding geometrical data are given in Table I.

larger than the length of a C=C double bond of about 1.31 Å, ¹⁵ but remarkably different from a single bond length of 1.58 Å. ¹⁵ Frauenheim and co-workers ⁷ find a dimer length of 1.41 Å which is slightly larger, whereas the the value of Gavrilenko of 1.66 Å differs appreciably from our result. On the other hand the latter author gives a value for the vertical distance between the first and second substrate layer $d_{12,\perp}$ which agrees with our result whereas the finding of Ref. 4 is smaller by about 12%. However, apart from this discrepancy our results are in close agreement with those obtained by means of the SLAB-MINDO method of Zheng and Smith. ⁴

Comparing the total energy of the ideal and the reconstructed surface we derive an energy gain of 3.52 eV per 2×1 surface unit cell. This is in reasonable agreement to the value of 3.0 eV obtained by Frauenheim et al. but much smaller than the formation energy of a C=C double bond of about 7.6 eV¹⁵ which is also given by semiempirical methods.⁴ The reason is that the near saturation of the surface dangling bonds by the formation of doubly bound symmetric dimers at the surface is accompanied by strain-induced rearrangements of the outermost substrate layers. As a result we find appreciable buckling amplitudes $\Delta_{3,\perp}$ and $\Delta_{4,\perp}$ in the third as well as fourth substrate layer (cf. Table I). This finding means that the released energy is partly compensated by the loss due to the lattice distortion in the subsurface layers. Comparing the total energy of the reconstructed C(100)2×1 surface and a bulk diamond slab we derive a cleavage energy of 2.29 eV per surface atom.

The self-consistent potentials obtained during the calculation allow us to determine the barrier seen by an electron passing from the bulk to the vacuum region. The ionization energy corresponds to the difference between this potential barrier and the valence-band maximum. We calculate an ionization energy of 6.0 eV for the reconstructed C(100) surface. This value is 1.6 eV smaller than that for the ideal surface.

electronic structure of the reconstructed $C(100)2\times1$ surface resulting within DFT-LDA is presented in Fig. 2(a). It is qualitatively similar to the band structure calculated for the $Si(100)2\times1$ surface. ^{16,18} The two surface bands within the fundamental gap are mainly related to dangling bonds pointing nearly parallel to the surface normal as can be seen from the wavefunction analysis in Fig. 3. Somewhat in contrast to the Si case the occupied (unoccupied) band is built up by bonding π (antibonding π^*) combinations of the dangling orbitals and not by single dangling bonds located at the upper (lower) dimer atoms. The surface bands related to the σ -dimer bonds occur within the projected bulk band structure. The pronounced π bonding and the nonoverlapping of the corresponding dimer wave functions with those of neighboring dimers (cf. Fig. 3) induce two further differences to the silicon case. There is a remarkable energy gap between occupied and unoccupied surface states already without buckling of the dimer. Moreover, measured in units of the fundamental gap the surface bands exhibit a smaller dispersion over the whole SBZ. The band maxima especially at the J'K line are less pronounced.

It is well known that the Kohn-Sham eigenvalues of the DFT-LDA have a restricted physical meaning. Hence, if they are taken to describe the one-electron energy spectrum, the resulting electronic excitation energies are generally seriously underestimated. An extreme example in this direction is the $C(111)2\times1$ surface, which appears to be metallic within the DFT-LDA picture. The underestimation of the band gaps also within our DFT-LDA calculation is obvious from the projected bulk band structure at the Γ point in Fig. 2(a). The experimental value of the bulk transition energy at Γ of about 6.0 eV²¹ is much larger than the DFT-LDA value of 4.05 eV. Consequently a proper treatment of electron exchange (X) and correlation (C) is essential to obtain accurate gap values.

This problem can be solved by treating the excitations within the quasiparticle (QP) Green's function formalism and calculating the XC self-energy Σ within Hedin's GW approximation.^{22,23} In this approximation the XC self-energy is replaced by the first-order term in the perturbational series with respect to the screened Coulomb potential W. Within the QP formalism one has to solve a Schrödinger-like equation, the so-called QP equation. In this equation the XC potential V_{XC} of the DFT-LDA is formally supplemented by the operator $\delta \Sigma = \Sigma - V_{\rm XC}$. The most important effect of $\delta\Sigma$ on the main peak in the spectral function is an energy shift $\delta \Sigma_{\nu}(\mathbf{k})^{24}$ since the QP wave functions are close to the corresponding DFT-LDA ones.²³ Thus the QP band structure results by adding these QP corrections $\delta \Sigma_{\nu}(\mathbf{k})$ to the Kohn-Sham eigenvalues of the DFT-LDA. In the surface case we write for the most important contribution:²⁵

TABLE I. Structural parameters (in Å) of the C(100)2×1 surface (cf. Fig. 1).

	$\Delta_{1,y}$	$d_{12,y}$	$d_{12,\perp}$	$d_{23,\perp}$	$d_{34,\perp}$	$d_{45,\perp}$	$\Delta_{3,\perp}$	$\Delta_{4,\perp}$
Present results	1.37	0.48	0.67	0.80	0.95	0.96	0.26	0.14
Ref. 4	1.38	0.52	0.59	0.80	0.94	0.94	0.25	0.15
Ref. 5	1.66	0.77	0.67	1.01	0.87	0.92	< 0.01	0.06

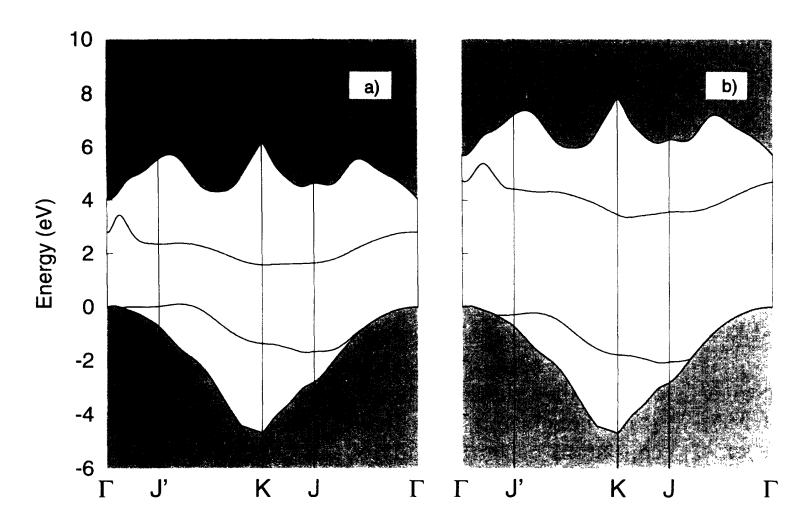


FIG. 2. DFT-LDA (a) and quasiparticle (b) band structure of the reconstructed $C(100)2\times1$ surface.

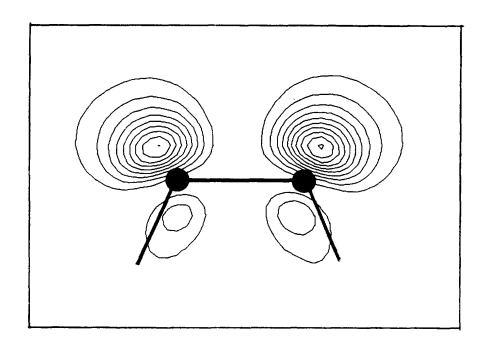
$$\delta\Sigma_{\nu}(\mathbf{k}) = \frac{1}{2F} \sum_{\mathbf{q}} \sum_{\mathbf{G}} \int \int_{-\infty}^{\infty} dz \ dz' \left[W(\mathbf{q} + \mathbf{G}, z, z') - W^{h}(\mathbf{q} + \mathbf{G}, z, z') \right]$$

$$\times \sum_{\mathbf{k}'} \sum_{\nu'} B_{\nu\nu'}^{\mathbf{k}\mathbf{k}'*}(\mathbf{q} + \mathbf{G}, z') B_{\nu\nu'}^{\mathbf{k}\mathbf{k}'}(\mathbf{q} + \mathbf{G}, z) \operatorname{sign}[\varepsilon_{\nu'}(\mathbf{k}') - \mu]$$
(1)

with two-dimensional (2D) Bloch integrals

$$B_{\nu\nu'}^{\mathbf{k}\mathbf{k}'}(\mathbf{Q},z) = \int d^2\mathbf{x}_{||}\varphi_{\nu\mathbf{k}}^*(\mathbf{x})e^{i\mathbf{Q}\mathbf{x}_{||}}\varphi_{\nu'\mathbf{k}'}(\mathbf{x}) \ . \tag{2}$$

In expressions (1) and (2) k and q denote wave vectors in the SBZ. G is a 2D reciprocal lattice vector. The



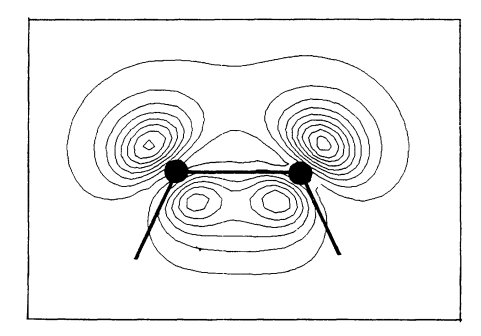


FIG. 3. Squared wave functions for $C(100)2\times1$ at the K point of the surface Brillouin zone (cf. Fig. 2). The upper (lower) panel shows the unoccupied (occupied) surface state. The contours are spaced by $0.01 \text{ e} \times \text{bohr}^{-3}$. The drawing plane contains the [100] and [110] axes.

real space vector \mathbf{x} is split into components parallel and perpendicular to the surface, $\mathbf{x}_{||}$ and z. $\varepsilon_{\nu}(\mathbf{k})$ is the energy eigenvalue of the band ν and μ is the chemical potential. $W(\mathbf{Q}, z, z')$ stands for the statically screened Coulomb potential of the truncated semiconductor, while $W^h(\mathbf{Q}, z, z')$ is that of the homogeneous electron gas.

In order to reduce the numerical effort in the surface calculations the self-energy operator is approximated as described and succesfully applied by Gygi and Baldereschi 26 for the bulk case. In the difference the XC potential V_{XC} is replaced by the QP self-energy of the homogeneous electron gas with the same average density, what is essentially the assumption of the LDA. The dynamical screening of the Coulomb potential W is replaced by the static one. Local-field contributions due to the atomic structure are neglected whereas those related to the surface are fully taken into account. To treat the screened Coulomb potential of the slab we make the assumption, that the influence of the surface states on the screening can be neglected.²⁷ Applying furthermore the approximation of specular electron reflection and truncating the polarization function at the electronic surface of the slab, we get an analytical expression of the screened Coulomb potential.^{25,28} In this expression two-dimensional Fourier transforms of the bulk screening function appear. The bulk screening function is replaced by a model function,²⁹ which is optimized with respect to full self-consistent random-phase approximation results.

The QP corrections are rather independent of the underlying DFT-LDA calculation. We take advantage of this fact by calculating QP corrections by means of a linear combination of atomic orbitals (LCAO) version of the DFT-LDA, ²⁰ which is more appropriate in the diamond case for numerical reasons. This method relies on the variational principle for the treatment of intra-atomic charge transfer, but incorporates a fully self-consistent treatment of interatomic charge transfer. The wave func-

tions in the matrix elements of the self-energy operator are expanded into a basis set of Gaussians localized at the carbon atoms. This enables us to calculate the Bloch integrals partly analytically, providing savings of a huge amount of computer time. Exchange and correlation are described according to Hedin and Lundqvist. The dispersion of the bulk bands given within this method is in good agreement with other theories. The bands have been found to have an indirect fundamental gap of 5.05 eV and a direct gap of 6.02 eV at Γ . However, these values are somewhat larger than those from other DFT-LDA approaches. 23

The resulting QP surface band structure together with the projected QP bulk band structure is shown in Fig. 2(b). The QP corrections shift the occupied LDA surface band down to lower energies (ranging from -0.79 eV near Γ to -0.88 eV at K) and the unoccupied surface bands towards higher energies (ranging from 1.47 eV at Γ to 1.25 eV at K). The surface band gap is therefore opened by 2.14–2.35 eV throughout the SBZ. In contrast to other surfaces like $C(111)2\times 1$ the QP correction of the gap varies rather weakly with k, in accordance with the small dispersion of the corresponding DFT-LDA bands. The QP corrections for the bulk bands, shifting the projected bulk band structure as well, are smaller than those of the surface states. The indirect gap is opened by 1.65 eV to a value of 5.7 eV. In Fig. 2(b) the valence-band maximum (VBM) is again used as energy zero. We find for the occupied surface band a maximum at 0.25 J'Knearly equal to the value of the VBM and a subsequent downwards dispersion of about 1.8 eV. It becomes a resonant state at about 0.2 $J\Gamma$. The unoccupied surface

band starting at 4.75 eV above VBM at Γ has a minimum near K of 3.3 eV above VBM. The gap between the surface states has its maximum at J with 5.6 eV and a minimum of 3.7 eV for the indirect transition 0.2 $J'K \longrightarrow K$. Despite the inclusion of the QP corrections the unoccupied π^* band remains in the forbidden region of the fundamental gap and, hence, forms a surface bound state. This finding is in contrast to those of Frauenheim et al.⁷ as well as Gavrilenko.⁵ In the non-self-consistent LCAO approach to the DFT-LDA only one occupied surface bound state has been observed in the lower half of the gap, whereas the self-consistent ETBM gives a practically filled dangling-bond state in the midgap region.

In conclusion, we have presented the first self-consistent ab initio study of the structural and electronic properties of the (100) surface of diamond. We find the symmetric dimer 2×1 reconstruction to be the ground state of the surface. The surface is stabilized by strongly σ - and π -bonded dimers. The QP band structure exhibits two well separated surface bands related to π - and π^* -dimer states within the fundamental gap. Taking into account QP corrections to the DFT-LDA bands both the gap between occupied and unoccupied surface bands and the fundamental gap are remarkably opened. Thereby the effect is slightly larger for the surface states.

We would like to thank D. Vanderbilt, M. Scheffler, R. Stumpf, and P. Käckell for their help with the computer codes. This work was financially supported by the Deutsche Forschungsgemeinschaft (Project No. Be1346/6-1) and by the EC Programme Human Capital and Mobility under Contract No. ERBCHRXCT 930337.

¹ A. V. Hamza, G. D. Kubiak, and R. H. Stulen, Surf. Sci. 237, 35 (1990).

² B. Sun, X. Zhang, and Z. Lin, Phys. Rev. B 47, 9816 (1994).

³ F. Bechstedt and D. Reichardt, Surf. Sci. 202, 83 (1988).

⁴ X. M. Zheng and P. V. Smith, Surf. Sci. **256**, 1 (1991).

⁵ V. I. Gavrilenko, Phys. Rev. B **47**, 9556 (1993).

⁶ S. H. Yang, D. A. Drabold, J. B. Adams, Phys. Rev. B 48, 5261 (1993).

⁷ T. Frauenheim, U. Stephan, P. Blaudeck, D. Porezag, H.-G. Busmann, W. Zimmerling-Edling, and S. Lauer, Phys. Rev. B 48, 18189 (1993).

⁸ J. E. Northrup, Phys. Rev. B **47**, 10032 (1993).

⁹ T. Tsuno, T. Imai, Y. Nishibayashi, K. Hamada, and N. Fujimori, Jpn. J. Appl. Phys. **30**, 1063 (1991); L. F. Sutcu, Appl. Phys. Lett. **60**, 1685 (1992).

¹⁰ B. Wenzien, P. Käckell, and F. Bechstedt, Surf. Sci. **307-309**, 989 (1994); P. Käckell, B. Wenzien, and F. Bechstedt, **50**, 10761 (1994).

¹¹ G.B. Bachelet, D.R. Hamann, and M. Schlüter, Phys. Rev. B **26**, 4199 (1982); L. Kleinman and D.M. Bylander, Phys. Rev. Lett. **48**, 1425 (1982).

¹² D.M. Ceperley and B.J. Alder, Phys. Rev. Lett. **45**, 566 (1980); J.P. Perdew and A. Zunger, Phys. Rev. B **23**, 5048 (1981).

¹³ R. Car and M. Parrinello, Phys. Rev. Lett. **55**, 2471 (1985).

¹⁴ R. Stumpf and M. Scheffler, Comput. Phys. Commun. 79, 447 (1994).

¹⁵ CRC Handbook of Chemistry and Physics, 74th ed. (CRC Press, Boca Raton, 1993).

¹⁶ J. Dabrowski and M. Scheffler, Appl. Surf. Sci. **56**, 15 (1992).

¹⁷ K. Kobayashi, Y. Morikawa, K. Terkura, and S. Blügel, Phys. Rev. B **45**, 3469 (1992).

¹⁸ D. Krüger and J. Pollmann, Phys. Rev. B 47, 1898 (1993).

¹⁹ F. Bechstedt, Adv. Solid State Phys. **32**, 161 (1992).

²⁰ D. Vanderbilt and S. G. Louie, Phys. Rev. **30**, 6118 (1984).

²¹ F. J. Himpsel, J. F. van der Veen, and D. E. Eastman, Phys. Rev. B 22, 1967 (1980).

²² L. Hedin and S. Lundqvist, Solid State Phys. 23, 1 (1969).

²³ M. S. Hybertsen and S. G. Louie, Phys. Rev. B **34**, 5390 (1986).

²⁴ F. Bechstedt, M. Fiedler, C. Kress and R. Del Sole, Phys. Rev. B **49**, 7357 (1994).

²⁵ C. Kress, M. Fiedler, and F. Bechstedt, Physica B **185**, 400 (1993).

²⁶ F. Gygi and A. Baldereschi, Phys. Rev. Lett. **62**, 2160 (1989).

²⁷ L. Reining and R. Del Sole, Phys. Rev. Lett. **67**, 3816 (1991).

²⁸ F. Bechstedt and R. Del Sole, Solid State Commun. **74**, 41 (1990).

²⁹ F. Bechstedt, R. Del Sole, G. Capellini, and L. Reining, Solid State Commun. **84**, 765 (1992); Phys. Rev. B **47**, 9892 (1993).

³⁰ L. Hedin and B.I. Lundqvist, J. Phys. C 4, 2064 (1971).

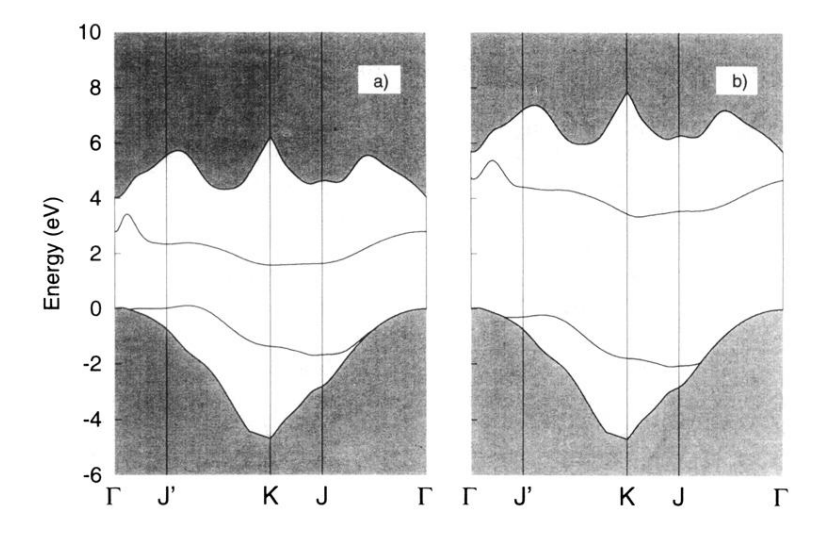


FIG. 2. DFT-LDA (a) and quasiparticle (b) band structure of the reconstructed $C(100)2{\times}1$ surface.